NASA TECHNICAL MEMORANDUM

NASA TM X-2319

NASA TM X-2319

JET PENETRATION INTO MACH 2 AIRSTREAM USING SWEPTBACK INJECTORS AT ANGLE OF ATTACK

by Martin Hersch and Louis A. Povinelli

Lewis Research Center
Cleveland, Ohio 44135

NATIONAL AERONAUTICS AND SPACE ADMINISTRATION • WASHINGTON, D. C. • JULY 1971

1. Report No.	2. Government Accession No.	3. Recipient's Catalog No.
NASA TM X-2319		

4. Title and Subtitle	5. Report Date
JET PENETRATION INTO MACH 2 AIRSTREAM USING SWEPTBACK INJECTORS AT ANGLE OF ATTACK	July 1971
	6. Performing Organization Code
7. Author(s)	8. Performing Organization Report No.
Martin Hersch and Louis A. Povinelli	E-6159
	10. Work Unit No.
9. Performing Organization Name and Address	722-03
Lewis Research Center National Aeronautics and Space Administration Cleveland, Ohio 44135	11. Contract or Grant No.
	13. Type of Report and Period Covered
12. Sponsoring Agency Name and Address	Technical Memorandum
National Aeronautics and Space Administration Washington, D. C. 20546	14. Sponsoring Agency Code

15. Supplementary Notes

16. Abstract

Helium was injected at sonic velocity normal to the leeward side of arrow- and delta-wing injectors. Vortex-controlling parameters including sweepback angle, swept-edge length, swept-edge wedge angle, and angle of attack were constant, but blockage and calculated drag were lower for the arrow injectors. The changes in vortex-enhanced penetration and lateral spreading were less rapid than the changes in blockage area and calculated drag. Also, helium, when injected from a porous area on the windward side, was swept over into the leeward vortex. Penetration in the vortex region was then greater than when helium was injected at sonic velocity directly into the vortex from the leeward side.

17. Key Words (Suggested by Author(s))

Vortex; Mixing; Supersonic; Delta wing; Jet penetration; Injection; Ramjet; Drag; Vapor screen; Visualization; Arrow wing; Porous; Angle of attack; Sweepback; Vortex; Flow

18. Distribution Statement

Unclassified - unlimited

19. Security Classif. (of this report)	20. Security Classif. (of this page)	21. No. of Pages	22. Price*
Unclassified	Unclassified	28	$3.00

*For sale by the National Technical Information Service, Springfield, Virginia 22151

JET PENETRATION INTO MACH 2 AIRSTREAM USING SWEPTBACK INJECTORS AT ANGLE OF ATTACK

by Martin Hersch and Louis A. Povinelli

Lewis Research Center

SUMMARY

It has previously been shown that vortices over the leeward surface of delta-wing injectors aid jet penetration and mixing into a supersonic stream. In this study the effects of injector blockage area and drag reduction on jet penetration were investigated using injectors having a sharp leading edge sweptback at 58.5° mounted at a 12° angle of attack in a Mach 2 airstream. Blockage and calculated drag were reduced by changing the planform from a delta- to an arrow-wing configuration. Vortex-controlling parameters, including sweepback angle, swept-edge length, swept-edge wedge angle, and angle of attack, were held constant. Helium was injected at sonic velocity from the leeward surface directly into the vortex region. A 36-percent reduction in blockage area was accompanied by a 20-percent reduction in jet penetration outside the vortex region. Penetration within the vortex region was unaffected. Lateral dispersion was reduced by about 12 percent.

The vortex motion originates from the windward surface and sweeps over the sweptback edge to the leeward surface; this suggests windward injection as a means of introducing injectant into the leeward vortex region. Accordingly, penetration measurements were also made with helium injected from a distributed source on the windward surface. At a 12° angle of attack no helium was detected in the leeward vortex region. At an 18° angle of attack the leeward vortex region was filled with helium. Leeward and windward injection were also compared using a symmetrical delta-shaped injector having two sharp leading edges sweptback at 75° mounted at a 22° angle of attack. Helium, when injected from a distributed source on the windward surface, completely filled one leading-edge vortex region. Roughly 50 percent greater penetration was obtained in the vortex region when compared to sonic injection directly into the vortex.

Free-stream total pressure and temperature of the Mach 2 airstream were 9.58×10^4 newtons per square meter (13.9 psia) and 347 K, respectively. Total helium injection pressure was 3.45×10^5 newtons per square meter (50 psia).

INTRODUCTION

Fuel injection into a supersonic stream is a critical problem in the development of the supersonic combustion ramjet engine. Satisfactory fuel-air mixtures may require injection from struts which protrude into the free stream, as opposed to injection from wall orifices. Townend (ref. 1) suggested that the struts might be designed to shed vortices into the injection and mixing regions. Such vortices, he proposed, would accelerate the process of mixing and dispersion of the fuel with the incoming airstream. The vortices would be generated by struts having sharp, sweptback leading edges at an angle of attack. The struts then would behave as delta wings at an angle of attack, the flow over which is well-known (described, for example, by Roy in ref. 2). Subsequent studies (refs. 3 to 5), have shown that fuel mixing and dispersion with a supersonic stream might indeed be improved by vortex-shedding injectors of delta-wing configuration.

Vortex size and strength are controlled by the sweepback angle, sweepback length, swept-edge wedge angle, and angle of attack. These parameters may be held constant while the blockage area is decreased by substituting an arrow for the delta planform as shown in the following sketches:

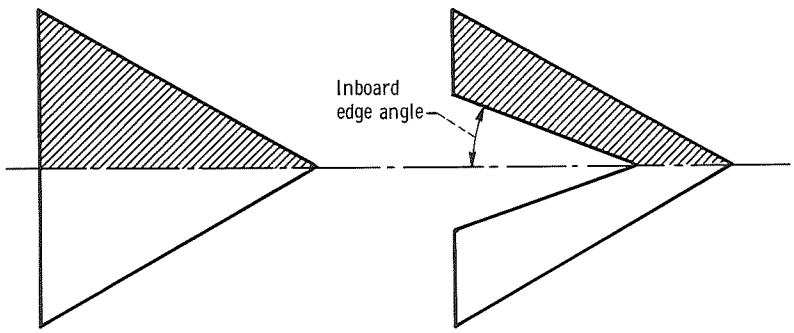

(a) Delta wing. (b) Arrow wing.

Therefore, one purpose of this study was to compare jet penetration of an arrow to a delta injector of equal sweepback angle, sweepback length, swept-edge wedge angle, and angle of attack. Penetration was determined as a function of blockage area. Blockage area was varied by changing the inboard edge angle shown in sketch (b). Semiplanform areas indicated by the shaded areas of the sketches were tested. Helium was injected at sonic velocity normal to the leeward surface of these injectors.

A second purpose of this study was to compare the effectiveness of windward injection from a distributed source to that of sonic injection from the leeward surface of swept injectors. In this portion of the study a full delta-wing configuration was also used. This injection technique was compared to leeward injection at sonic velocity.

APPARATUS AND PROCEDURE

Wind Tunnel and Injectors

All tests were conducted in the Mach 2, 9.75- by 25.4-centimeter wind tunnel described in reference 3. Planforms, a typical cross section, and an edge view of the injectors used for studying the effects of blockage area and drag reduction are shown in figure 1. The sweepback angle, overall length, and thickness (at the trailing edge) of these injectors were 58.5°, 7.68, and 1.08 centimeters, respectively. Area was changed by varying the inboard edge angle shown in figure 1. If lines through the apexes are considered to be lines of symmetry, then configuration A is seen to be one-half of a delta wing, and configurations B to D, one-half of arrow wings. Areas of configurations B to D are 89, 77, and 64 percent of configuration A. The inboard portions removed are assumed to be unimportant for vortex generation. Injection orifice diameter was 0.198 centimeter. Configuration A, the semidelta injector, was also used in the studies of reference 4.

All the injectors had subsonic leading edges for the test conditions used. The component of a Mach 2 free stream normal to the 58.5° sweptback leading edge at a 12° angle of attack is 1.10. However, the sum of the wedge angle of the leading edge (24.8°) and the angle of incidence of the component normal to the leading edge is such that the leading-edge shock wave is detached. Hence, circulation occurs from the windward to the leeward side of the injectors and gives rise to vortex motion.

Measurements were also made by using a symmetrical full delta configuration shown in figure 2. This injector had two sharp leading edges with sweepback angles of 75° and was mounted at a 22° angle of attack.

Helium was also injected from the windward side of configuration C (fig. 3) and the symmetrical full delta injector. Windward injection was from a sintered porous metal strip flush with the surface, as shown in figures 2 and 3. The porosity of the metal was 43.6 percent, based on the density ratio of sintered to solid metal.

In this study, downstream distance, denoted by x, is measured from the injection orifice location parallel to the undisturbed free stream. Lateral distance, denoted by z, except as noted, is also measured from the orifice location, normal to the free stream, with the positive direction towards the sweptback edge. The third dimension, denoted by y, is measured from the injector surface in a direction perpendicular to the undisturbed free stream. For the case of measurements downstream of the trailing edge, y is measured from the projection of the leeward trailing edge parallel to the free stream. These distances are nondimensionalized by the injection orifice diameter d. (Symbols are defined in appendix A.)

Operating Conditions

The free-stream Mach number, total pressure, and temperature were 2, 9.58×10^4 newtons per square meter (13.9 psia), and 347 K, respectively. Total injection pressure for all tests was 3.45×10^5 newtons per square meter (50 psia). Injectant mass flow was controlled by the total pressure and sonic flow through the leeward injection orifice, or the internal passage of the injector in the case of windward injection. Since the diameters of the sonic restrictions were nearly equal for all injectors, injectant mass flow was nearly constant throughout the tests.

Flow Visualization

The flow over the injector surfaces was visualized by use of the vapor-screen technique which is described in reference 6. For this purpose the tunnel was operated with moist unheated air drawn in directly from the atmosphere. The moisture condensed to form a dense fog in the test section. This was illuminated by a sheet of light from a mercury arc perpendicular to the axis of the tunnel. Any disturbance in the flow through this plane disturbs the uniform distribution of fog particles, and hence the amount of light scattered by the fog. These disturbances, such as vortices, appear as dark regions on a brilliant screen. This technique is useful for providing rapid qualitative evaluation of the flow field, vortex location and shape, and jet penetration.

Pressure and Concentration Measurement

The probe used for pitot pressure measurement or gas sampling had a 0.086-centimeter-diameter opening. The probe was traversed in the y-direction. Pitot pressure or helium concentration profiles in the y-direction were recorded as a function of probe position on an x,y-plotter. The z-positions of the traverses were varied by rotating the probe at an angle of yaw. Thus, series of profiles were obtained which were crossplotted to obtain pressure or concentration contours in the y,z-plane. The variation of the probe tip position in the x-direction due to rotation was approximately 1 jet diameter. Pitot pressure was measured without injection. Helium concentration was determined with a mass spectrometer as described in reference 3.

Measurements were made an x/d-position of 19.4 for configurations A to D at a 12° angle of attack, and at an x/d-position of 13.1 for configuration C at an 18° angle of attack. The x/d-positions of the measurements using the full delta injector varied from 15.9 to 29.5.

RESULTS AND DISCUSSION

Injector Drag

A first-order approximation of drag was calculated as shown in appendix B for configurations A to D. The induced, friction, and thickness drag coefficients are shown in figure 4 as a function of angle of attack and the thickness ratio δ_e. In figure 5, wave and friction drag, nondimensionalized by that of configuration A, is plotted against relative planform area for a 12^o angle of attack. It is noted in figure 4 that the thickness ratio for the injectors varied from 0.25 to 0.39 for configurations A to D. Had the injectors been of equal thickness ratio, the wave drag would simply have been proportional to planform area, as shown by the curve in figure 5. Since vortex size and strength are functions of sweepback angle, swept-edge length, swept-edge wedge angle, and angle of attack (ref. 7), it is reasonable to assume that the vortex enhancement of jet penetration does not depend upon injector thickness ratio. Hence, it is expected that injectant distribution measurements made in this study would apply to injectors of both equal and unequal thickness ratio.

Vapor-Screen Observations

Vapor-screen observations were made for all injectors. Vapor-screen photographs for injector configuration C are shown in figure 6. Figure 6(a) shows the injector mounted in the tunnel with no flow and normal illumination. Figure 6(b) shows the vapor screen slightly upstream of the injector trailing edge with a Mach 2 free stream and no injection, and figure 6(c), the appearance with helium injection. The vortex shed by the sweptback leading edge appears as a broad flat dark area over the leeward surface. Evidence of a small vortex trailing from the tip and inboard edge is also seen. This vortex was completely separated from the leading-edge vortex, was outside of the field of measurement, and was not considered in the present study. The intersection of the conical shock generated by the tip and leading edge with the vapor-screen plane is also visible.

Visual vapor-screen observations, not photographed, for the symmetrical full delta injector showed two roughly circular dark regions above the leeward surface. These indicated the presence of a pair of leading-edge vortices, one generated by each sweptback edge.

With helium injection, figure 6(c), a faint, vertically elongated dark region appears near the inboard edge directly downstream of the injection orifice. As will be shown by concentration measurements, this dark region which only appears with helium injection results from injectant which is not captured by the vortex, but flows directly downstream from the orifice.

Pitot Pressure Contours

Pitot pressure isobars in the leeward flow field over the various injectors are shown in figures 7 and 8. In figure 8, z is measured from the injector centerline rather than from the orifice. The contour patterns agree with the qualitative vapor-screen observations. A horizontally elongated low-pressure region extends over the leeward surface of configurations A to D. This represents the location and shape of the leading-edge vortex. Some of the contours also indicate the presence of the smaller vortex shown on the vapor screen, which trails downstream from the tip ($z/d \approx -2$).

The vortex size, inferred from the pitot pressure contours, appears to be nearly independent of the area reductions of configurations A to C. Configuration D begins to reduce the vortex size. The contour also suggests flow circulation around the inboard edge.

The contours for the symmetrical delta wing, figure 8, show two nearly circular low-pressure regions, each of which indicates the position of a leading-edge vortex.

Helium Concentration Distribution

Helium concentration contours measured for configurations A to D are shown in figure 9. These patterns all show the skewed, asymmetrical shape noted in references 3 and 4. As noted in references 3 and 4, one portion of the helium jet is not captured by the vortex, but flows directly downstream from the orifice, as if injection were from a flat plate with no vortex motion present. The other portion of the helium is captured by the vortex and does not penetrate as deeply into the free stream as the first portion, but is spread out laterally by the vortex in the region $6 \lesssim z/d \lesssim 18$.

The jet from injector D does not flow directly downstream from the orifice, but is deflected towards the vortex region. This deflection may have been caused by flow expansion over the inboard edge of this injector. The lateral dispersion with this injector was therefore somewhat less than with the other configurations.

Helium penetration in the region of maximum penetration ($z/d \approx 0$) and in the vortex region ($6 \lesssim z/d \lesssim 18$) is shown as a function of relative injector area and drag in figure 10. Two drag scales are shown. In the upper scale, the thickness drag coefficient is constant, so drag is proportional to projected planform, as shown in figure 5. The calculated drag is shown on the lower scale, which takes into account the variable-thickness drag coefficient shown in figure 5.

Each vertical bar represents three, or in the case of configuration D, four sets of measurements. Experimental scatter appears to be approximately ±1 jet hole diameter.

Directly downstream of the injector orifice, penetration decreased from 8.1 jet diameters for configuration A to 6.5 for configuration D. Thus, blockage area and drag (neglecting variation of injector thickness ratio) were reduced 36 percent with a 20-percent

decrease in helium penetration outside the vortex region. However, within the vortex region, penetration is nearly independent of injector configuration.

Lateral helium distribution is shown in figure 11. The maximum decrease in lateral distribution is approximately 12 percent. Most of the decrease occurs between injector configurations C and D. This suggests that the area reduction of configuration D begins to influence the vortex flow region.

In reference 5, it was noted that the jet, located on the leeward surface, appeared to disrupt the vortex. Vortex disruption may partially negate the full potential of vortex mixing. The disruption may be due to high-velocity components of the jet which are not oriented properly with the vortex motion. This suggests modifying the injection technique so that the vortex efficiently entrains the injectant, but is not disrupted. Townend (ref. 1), proposed injection from the leading edges of sweptback injectors. Since the vortex motion originates from the windward surface and sweeps over the leading edge to the leeward surface, an alternate technique might be injection from a distributed source on the windward surface.

One injector, configuration C, was therefore modified for windward injection from a distributed source. The leeward orifice was sealed, and helium was injected from the porous sintered metal strip shown in figure 3.

At an angle of attack of 12° no helium was detected over the leeward surface. At an 18° angle of attack the vortex region was filled with helium as shown in figure 12. The helium was confined to the vortex region and none was detected directly downstream of the injection orifice at $z/d = 0$. Maximum penetration of helium over the leeward surface was 4 jet diameters. With leeward injection at a 12° angle of attack, penetration in this region was about 2.5 jet diameters (fig. 9(c)). Leeward injection was not measured at an 18° angle of attack. However, the results of reference 4 indicate that penetration in the vortex region, using leeward injection, would not almost double in going from a 12° to an 18° angle of attack.

It is noted that the helium distribution does not extend to the leading edge. In reference 4 it was found that flow separation occurred near the downstream region of the sweptback edge at an 18° angle of attack. This explains the absence of helium near the leading edge at the x/d station of 13.1, which is in the area of separation.

The pressure differential from the windward to leeward surfaces increases with increasing angle of attack. The complete absence of helium in the vortex region at a 12° angle of attack therefore suggests that a minimum angle of attack is required for vortex capture of gas injected from the windward surface. This minimum angle of attack for this injector was not determined.

Helium Distribution From Symmetrical Delta Injector at 22° Angle of Attack

Helium distribution patterns resulting from leeward or windward injection from the symmetrical delta-wing injector are shown in figures 13 and 14. As with the asymmetrical sweptback injectors, a large portion of the helium, when injected from the leeward surface, is not captured by the vortex, but flows directly downstream from the injection orifice (fig. 13) in the region $0 < z/d < 3$. Also, even though helium was injected into only one vortex, it has entered both leading-edge vortices, probably by crossflow on the plate surface. These results indicate that inefficient vortex capture of injectant may not be attributed to injector asymmetry, such as that of the half delta configurations.

Helium distributions at three x/d stations with windward injection from the porous strip of the symmetrical delta-wing injector are shown in figure 14. In figure 14, z is measured from the injector centerline. High helium concentrations were detected in one of the leading-edge leeward vortices. Helium did not cross the injector centerline upstream of the trailing edge.

A comparison of the jet boundary location for leeward and windward injection using the symmetrical injector at a 22° angle of attack is shown in figure 15. Penetration in the vortex region only is compared here; the injectant which was not captured by the vortex was neglected. These results show that, when the symmetrical delta-wing injector is used, greater penetration in the vortex region is achieved for windward than leeward injection. In the vicinity of the trailing edge the penetration gain in the vortex region is greater than 50 percent. Also shown in figure 15 are the vortex core positions indicated by pitot pressure measurements with no injection.

Windward injection might be a useful technique for injector cooling. The greatest heat load on a delta-wing injector at an angle of attack in a supersonic stream is on the windward surface and leading edges. As shown in this study, it is these areas which are sheathed by cool gas when injection is from the windward surface.

CONCLUSIONS

Jet penetration into a Mach 2 airstream was investigated by using vortex injectors having a sharp sweptback leading edge at an angle of attack. One purpose of this study was to determine the effects on jet penetration when the injector blockage area and drag were reduced. The area blockage reduction was achieved by removing portions of the injector which do not contribute to vortex generation. For a 36-percent reduction in blockage area, jet penetration outside of the vortex region was reduced by about 20 percent, and lateral dispersion was reduced by about 12 percent. Most of the loss in lateral spreading occurred for area reductions greater than 23 percent.

The effects of varying the location of injection were also investigated. The results just mentioned were obtained with leeward injection from a sonic orifice on the leeward surface. With this injection technique the vortex is disrupted, and portions of the jet are not entrained by the vortex. Therefore, helium was also injected from a distributed source on the windward surface. When this injection method was used, a high concentration of helium was found in the leading-edge vortex over the leeward surface. Penetration in the vortex region was greater when this technique was used than it was with injection at sonic velocity directly into the vortex region on the leeward surface. Also, a minimum angle of attack, or pressure differential, is required for injectant flow from the windward to leeward regions. Windward injectant from a distributed source might also be a useful cooling technique, because those portions of the injector subject to high aerodynamic heating, the leading edge and windward surface, can be sheathed by cool injectant.

Lewis Research Center,
National Aeronautics and Space Administration,
Cleveland, Ohio, April 5, 1971,
722-03.

APPENDIX A

SYMBOLS

A	planform area
C_D	drag coefficient, $D/(1/2\rho_\infty V_\infty^2 A)$
D	drag force
d	orifice diameter
L	swept-edge length
l	chord length
M	Mach number
p	static pressure
t	injector thickness
V	velocity
x	downstream distance
y	distance from injector surface perpendicular to undisturbed free stream
z	lateral distance
α	angle of attack
δ	thickness ratio, t/l
Λ	wing sweepback angle
ρ	density

Subscripts:

b	base
e	direction normal to leading edge
i	induced
in	inboard
psa	projected side area
te	trailing edge
th	thickness
∞	free stream

APPENDIX B

DRAG CALCULATION

An estimate was made of the drag of the four models tested (A, B, C, and D). It was assumed that the models were infinite wings having a constant chord length. The component of the chord normal to the leading edge ($l \cos \Lambda$) was assumed to be equal to the chord length at the midpoint of the swept edge of the delta wing. The idealized configuration used for the calculations is shown in figure 16(a).

A plan view of the infinite sweptback wing is shown in figure 16(b) and cross-sectional views in figures 16(c) and (d). The induced drag was determined from the following expression (ref. 8):

$$C_{D,i} = C_{D,i,e} \cos \Lambda \left(1 - \sin^2 \Lambda \cos^2 \alpha\right)$$

where

$$C_{D,i,e} = 4\alpha_e^2 \Big/ \sqrt{M_{\infty,e}^2 - 1}$$

$$\alpha_e = \arctan\left(\frac{\tan \alpha}{\cos \Lambda}\right)$$

and

$$M_{\infty,e} = M_\infty \sqrt{1 - \sin^2 \Lambda \cos^2 \alpha}$$

The thickness drag coefficient $C_{D,th}$ was determined from

$$C_{D,th} = C_{D,th,e} \cos \Lambda \left(\frac{M_{\infty,e}}{M_\infty}\right)^2$$

where

$$C_{D,th,e} = 2\delta_e^2 \Big/ \sqrt{M_{\infty,e}^2 - 1}$$

and

$$\delta_e = t/l \cos \Lambda = \delta/\cos \Lambda$$

The skin-friction drag coefficient was assumed to have a constant value of 0.006. The contribution of the skin-friction drag to the drag ratio was only 1/2 percent.

The drag ratio was determined from the summation of the drag coefficients multiplied by the appropriate area of the four injectors. The drag was nondimensionalized by the calculated drag of model A to give the drag ratio D/D_o.

For an angle of attack of 12^o, figure 5 shows the following values:

Model	Drag coefficient, C_D	Area ratio, A/A_o	Drag-force ratio, D/D_o
A	0.27	1.0	1.0
B	.29	.89	.95
C	.31	.77	.89
D	.36	.64	.84

The base drag was also calculated for the four models but not included in the preceeding table since it only changes the D/D_o values by 4 percent. When the base drag was calculated, it was assumed that a Prandtl-Meyer expansion occurred over the trailing edge (90^o expansion) and around the inboard edge (model A, 0^o expansion; B, 5.7^o; C, 10.3^o; and D, 16.5^o). The base drag was then determined from the expression

$$D_b = (P_\infty - P_{te}) A_b + (P_\infty - P_{in}) A_{psa}$$

For model A the second term is zero.

The nonlinear effects of the vortex motion and the effects of injection may be significant in determining the injector drag. A calculation of this type was, however, not feasible.

REFERENCES

1. Townend, L. H.: Ramjet Propulsion for Hypersonic Aircraft. Rep. TM-Aero-917, Royal Aircraft Establishment, Jan. 1966.

2. Roy, Maurice: On the Theory of the Delta Wing Vortices From the Apex and Sheets in Cornet. Rech. Aero., no. 56, Feb. 1957. (Also available as translated by Snyder, Melvin H., Jr.: On the Theory of the Delta Wing. Aero. Rep. 66-4, Wichita State Univ., Sept. 1966.)

3. Povinelli, Louis A.; Povinelli, Frederick P.; and Hersch, Martin: A Study of Helium Penetration and Spreading in a Mach 2 Airstream Using a Delta Wing Injector. NASA TN D-5322, 1969.

4. Povinelli, Frederick P.; Povinelli, Louis A.; and Hersch, Martin: Effect of Angle of Attack and Injection Pressure on Jet Penetration and Spreading From a Delta Wing in Supersonic Flow. NASA TM X-1889, 1969.

5. Hersch, Martin, and Povinelli, Louis A.: Effect of Interacting Vortices on Jet Penetration Into a Supersonic Stream. NASA TM X-2134, 1970.

6. McGregor, I.: The Vapour-Screen Method of Flow Visualization. J. Fluid Mech., vol. 11, p. 4, Dec. 1961, pp. 481-511.

7. Pershing, Bernard: Separated Flow Past Slender Delta Wings With Secondary Vortex Simulation. Rep. TDR-269 (4560-10) -4, Aerospace Corp. (SSD-TDR-64-151, DDC no. AD-607442), Aug. 24, 1964.

8. Shapiro, Ascher H.: The Dynamics and Thermodynamics of Compressible Fluid Flow. Vol. II. Ronald Press Co., 1953.

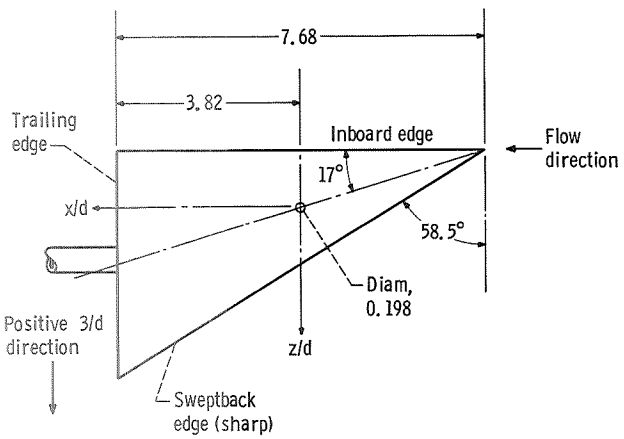

Configuration A

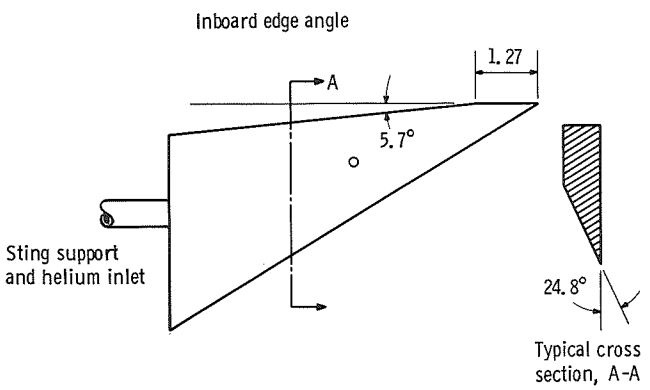

Configuration B

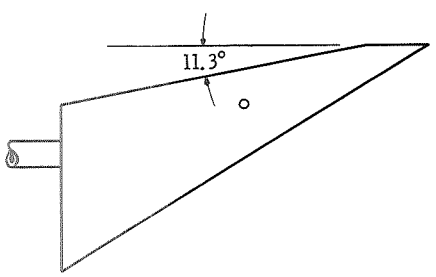

Configuration C

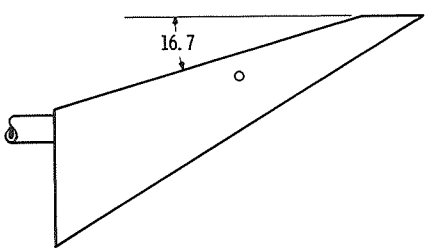

Configuration D

(a) Planform views (viewed normal to leeward surface).

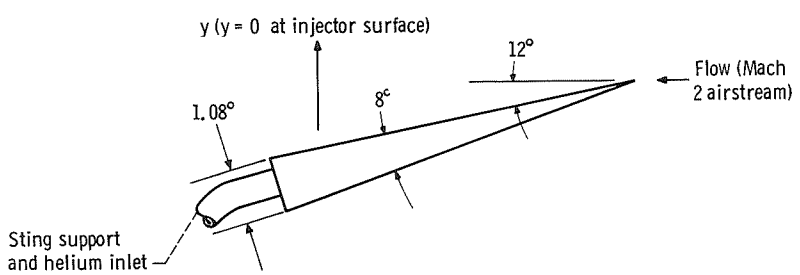

(b) Side view.

Figure 1. - Delta and arrow wing injectors. (Dimensions in cm.)

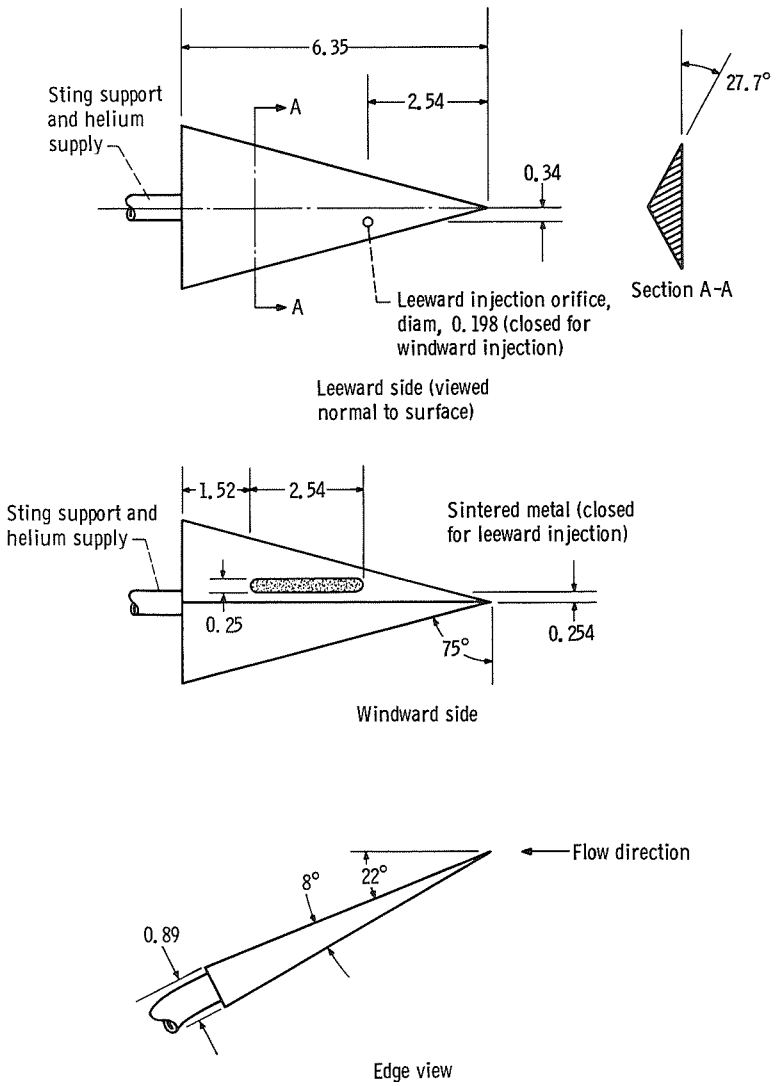

Figure 2. - Symmetrical full delta injector. (Dimensions in cm.)

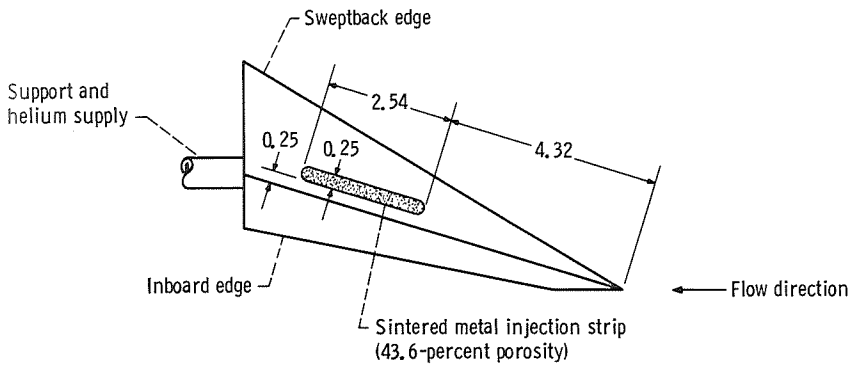

Figure 3. - Windward view of injector configuration C showing sintered injection strip. Angle of attack, 18°.

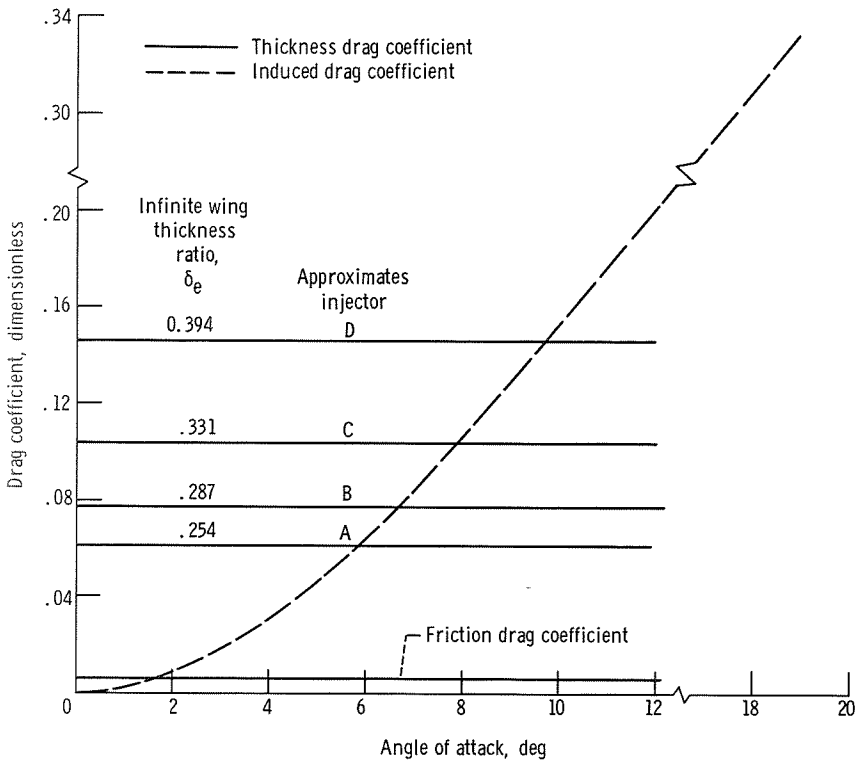

Figure 4. - Linear calculated drag coefficient for infinite wing.

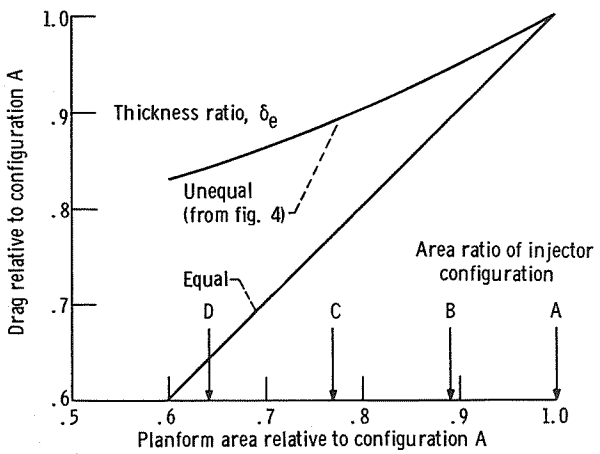

Figure 5. - Injector drag as function of area at 12^0 angle of attack.

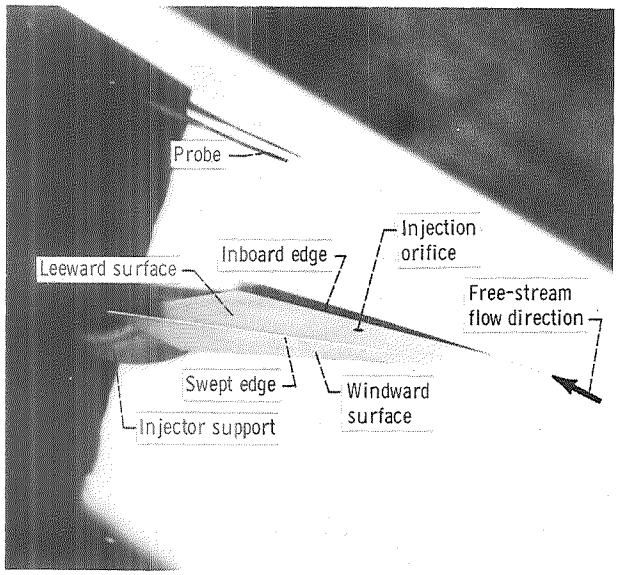

(a) No flow, normal illumination.

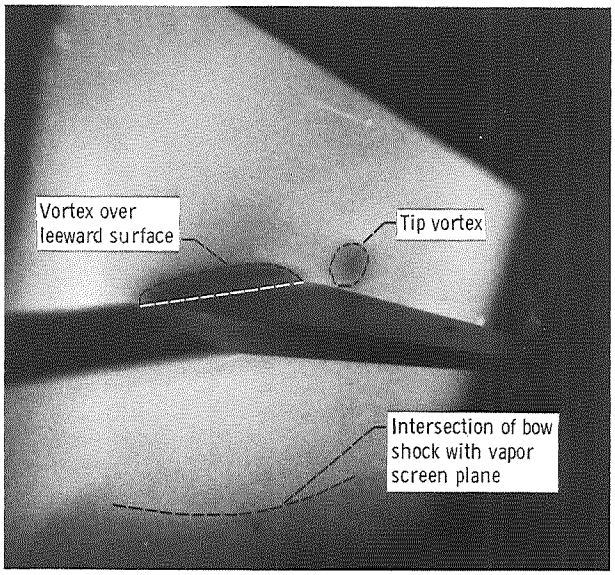

(b) Mach 2 free-stream flow; no injection.

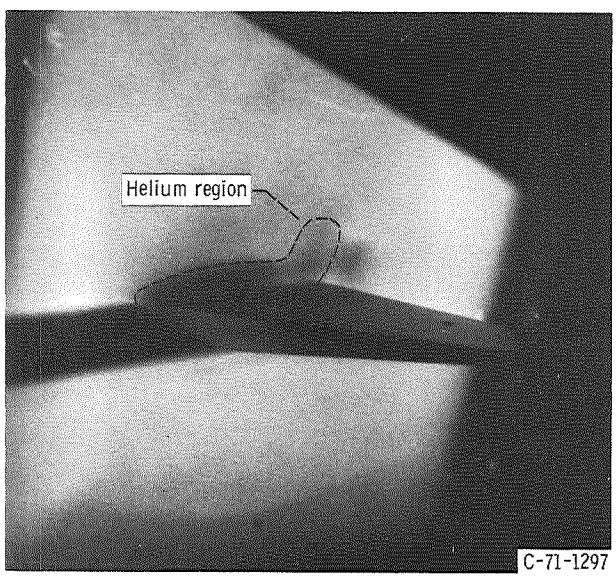

(c) Mach 2 free-stream flow; helium injection.

Figure 6. - Configuration C mounted in tunnel for vapor-screen photography.

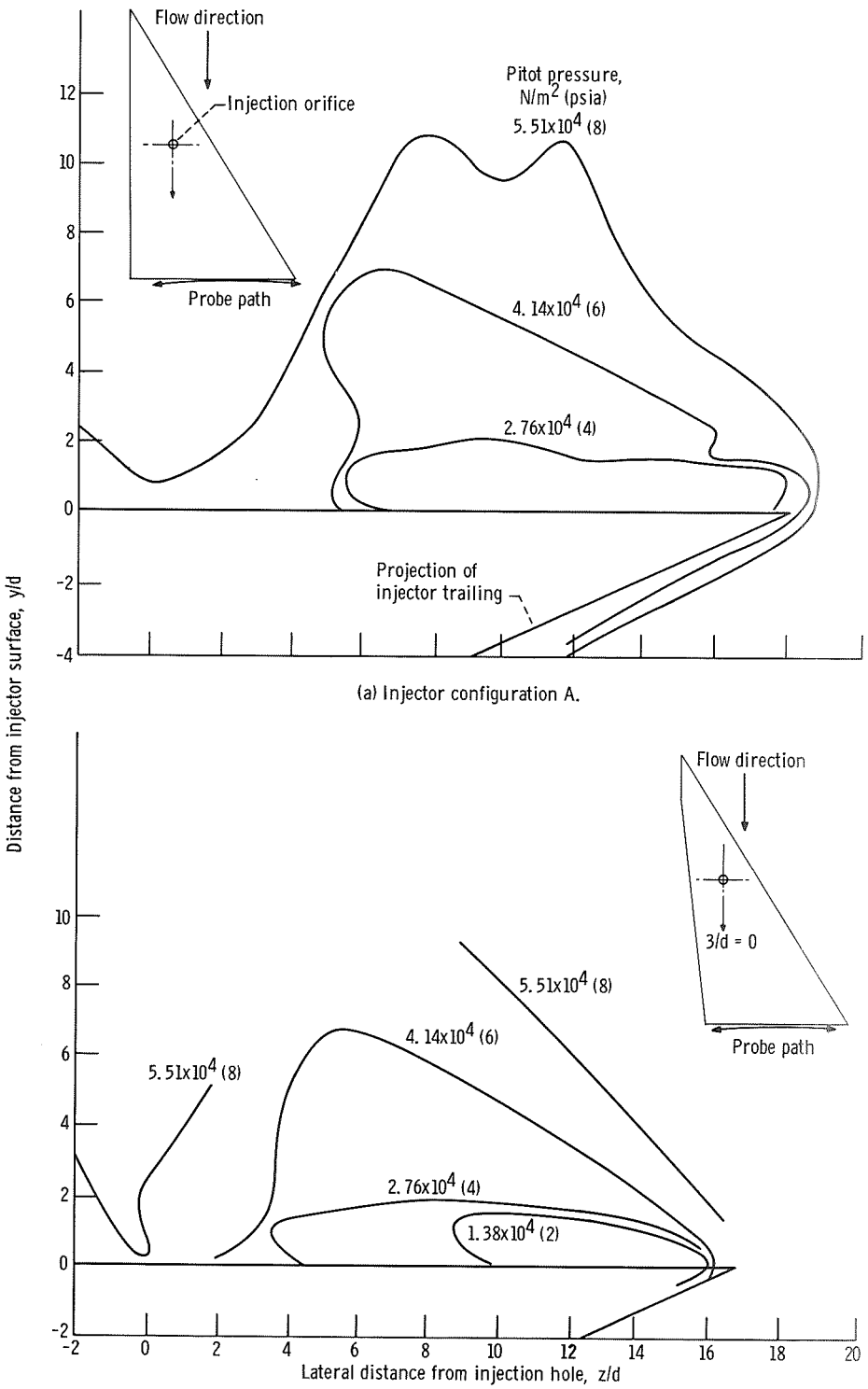

Figure 7. - Pitot pressure contours. Distance downstream from injector orifice, 19.4; sweepback angle, 58.5°; angle of attack, 12°; no injection.

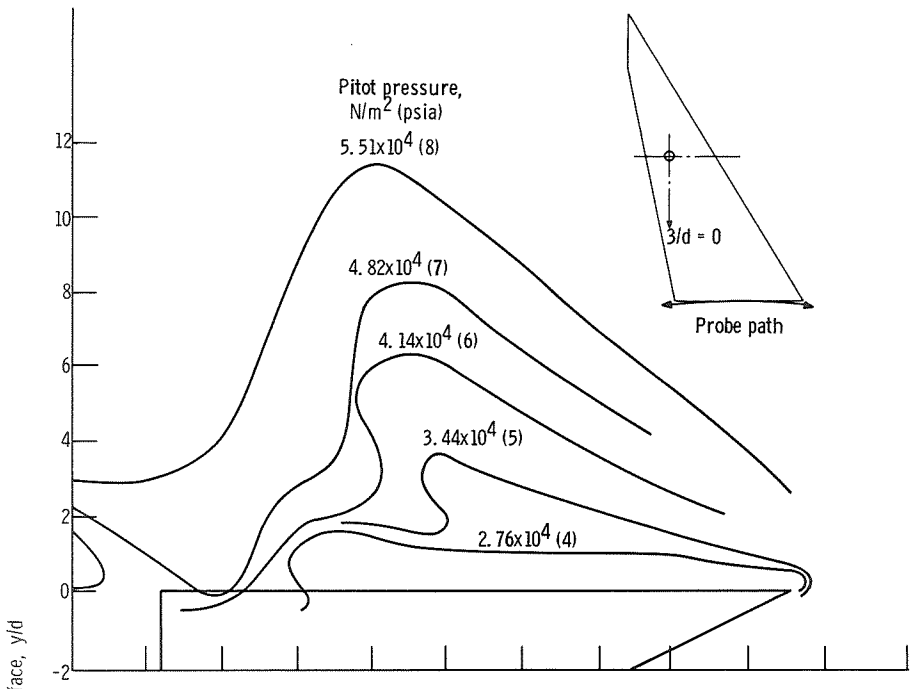

(c) Injector configuration C.

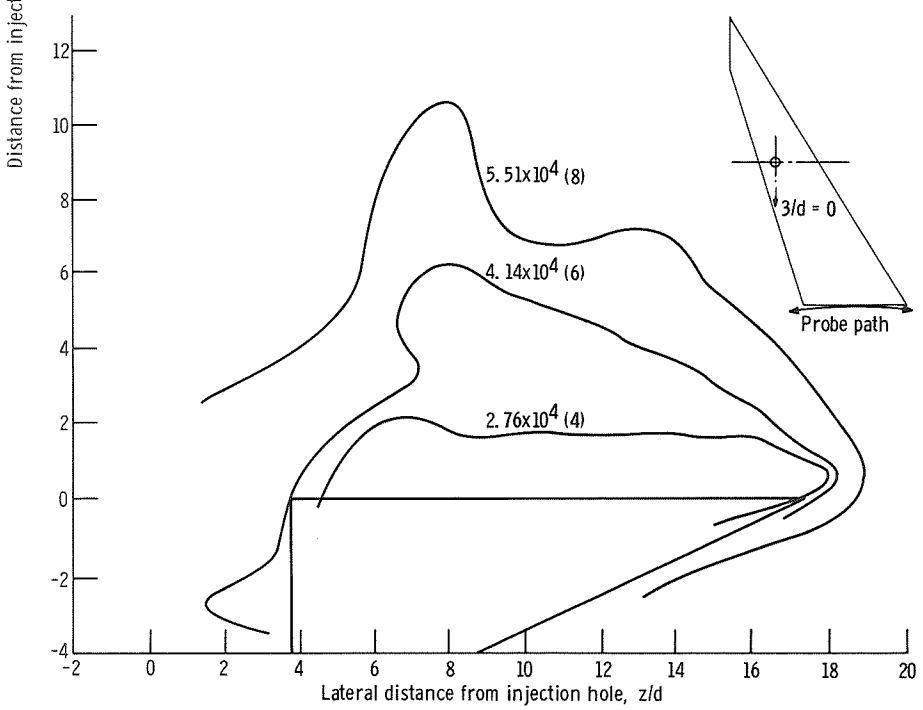

(d) Injector configuration D.

Figure 7. - Concluded.

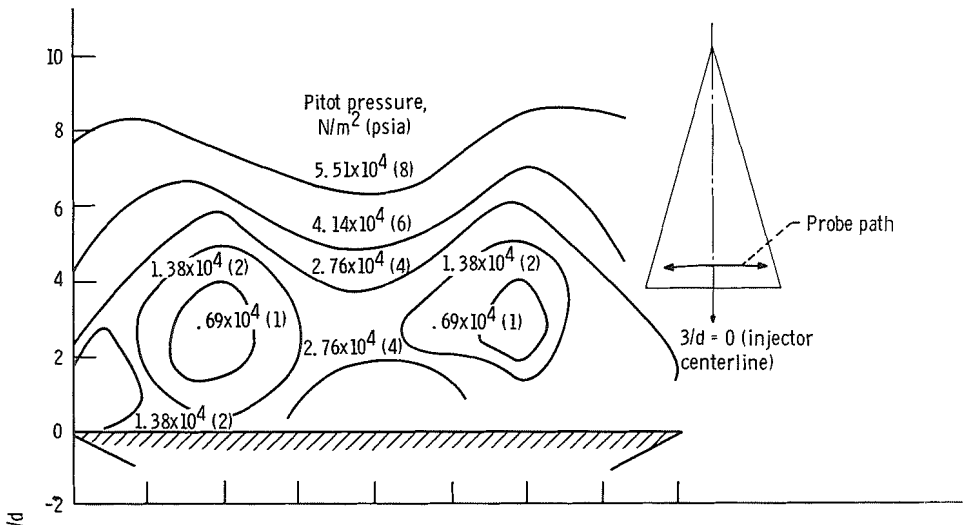

(a) Distance downstream from injector orifice, 15.9; no injection.

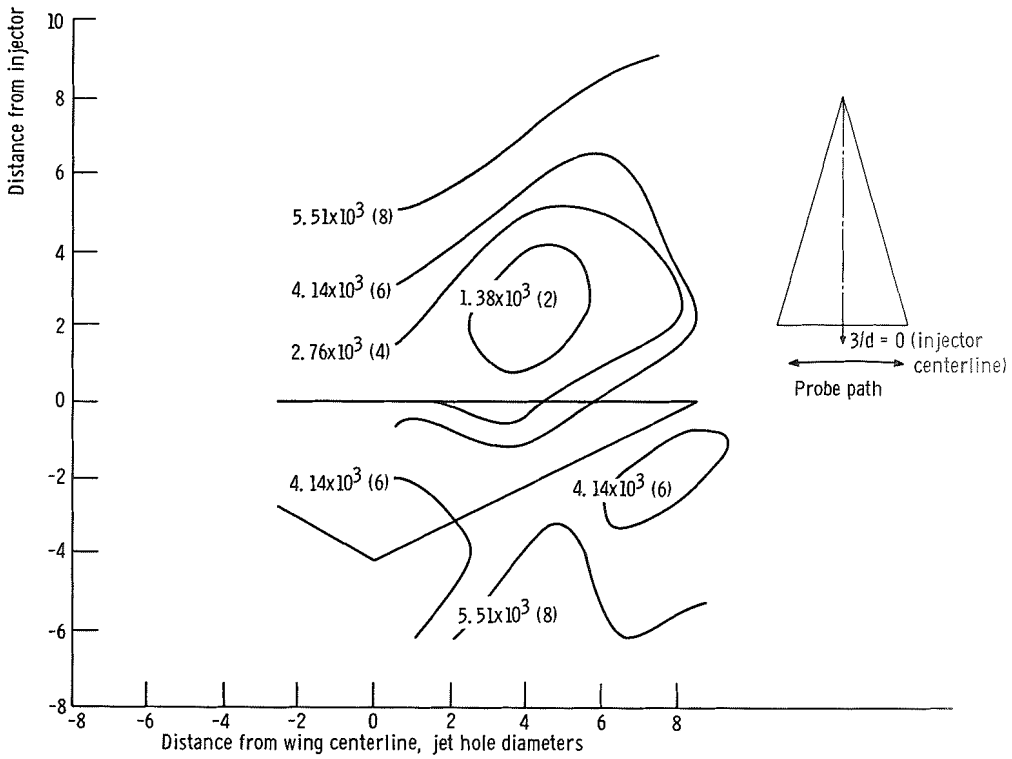

(b) Distance downstream from injector orifice, 29.5; no injection.

Figure 8. - Pitot pressure contours. Symmetrical delta wing injector: sweepback angle, 75°; angle of attack, 22°.

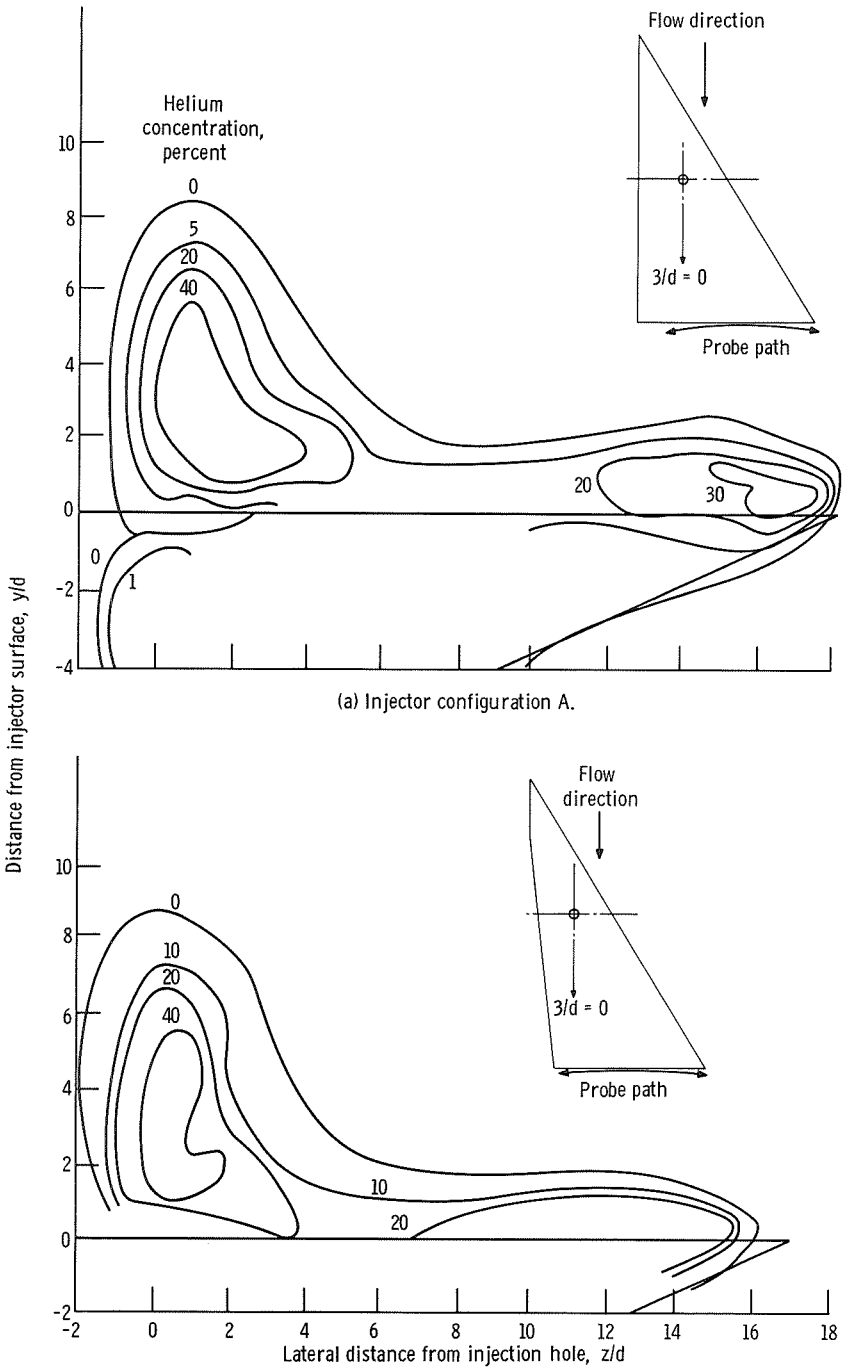

Figure 9. - Helium distribution. Distance downstream from injector orifice, 19.4; sweepback angle, 58.5°; angle of attack, 12°.

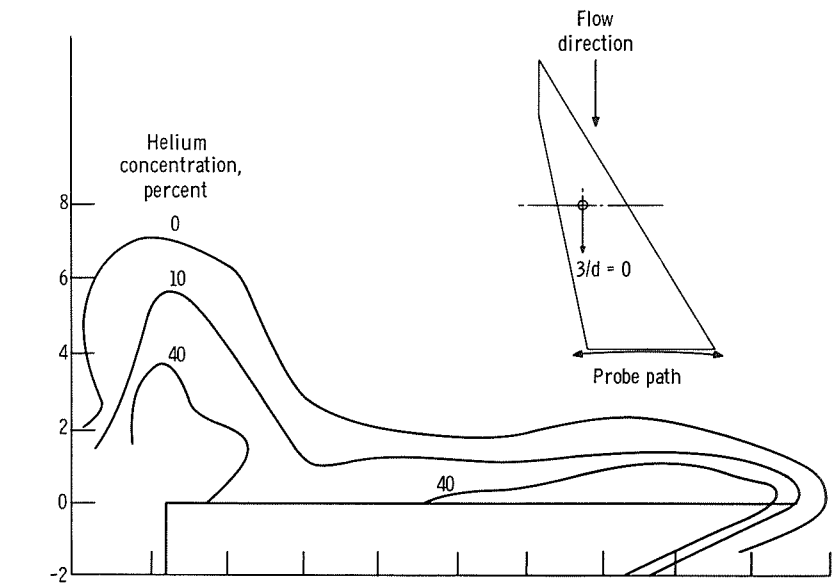

(c) Injector configuration C.

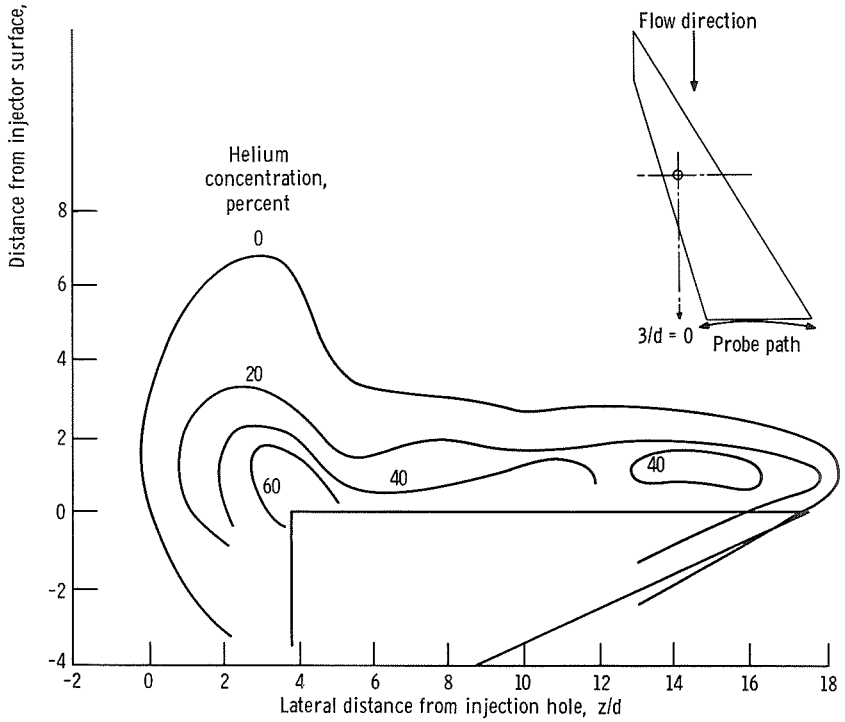

(d) Injector configuration D.

Figure 9. - Concluded.

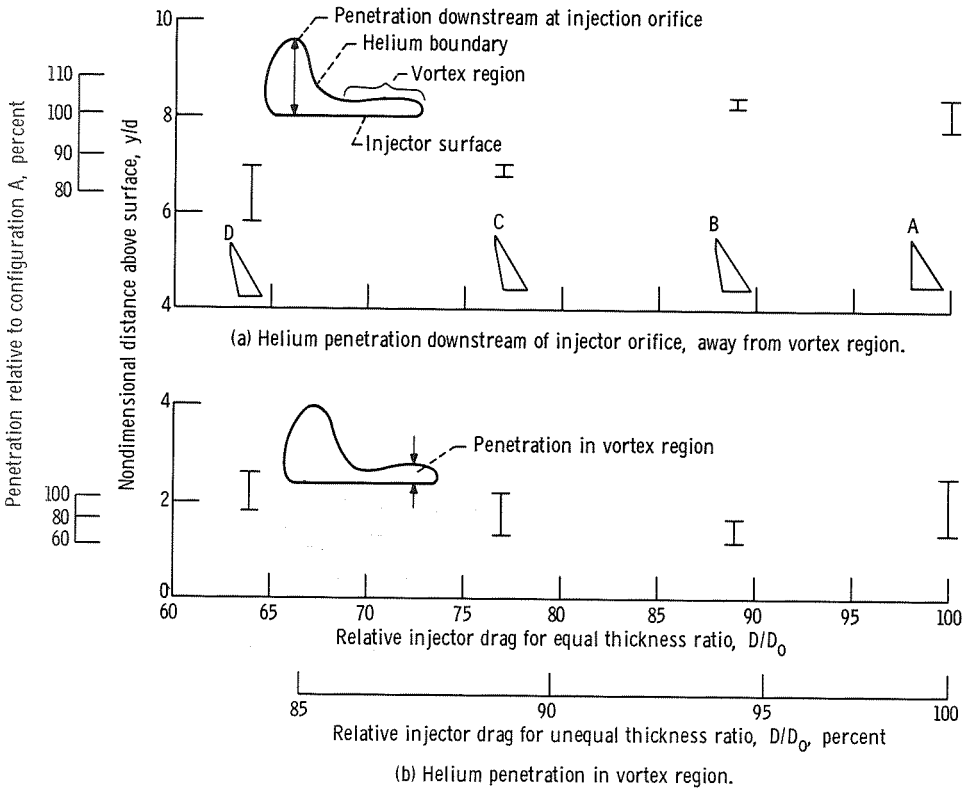

Figure 10. - Helium penetration downstream of orifice and in vortex region. Sweepback angle, 58.5°; angle of attack, 12°; distance downstream from injector orifice, 19.4.

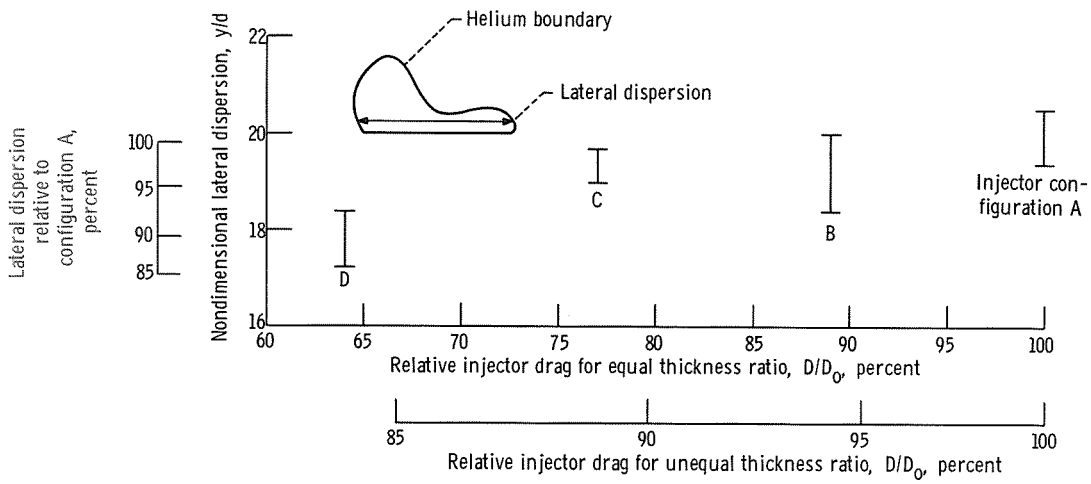

Figure 11. - Lateral helium dispersion. Sweepback angle, 58.5°; angle of attack, 12°; distance downstream from injector orifice, 19.4.

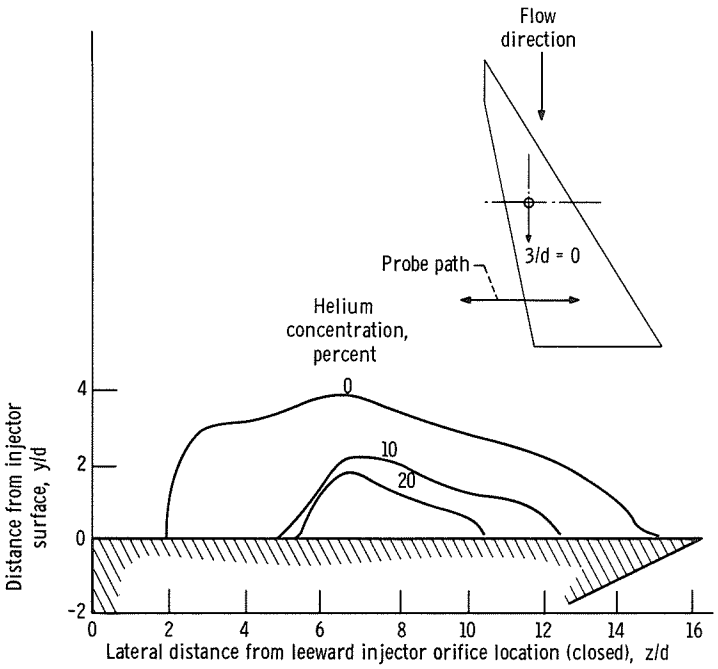

Figure 12. - Helium distribution for windward injection from injector configuration C. Distance downstream from injector orifice, 13.1; sweepback angle, 58.5°; angle of attack, 18°.

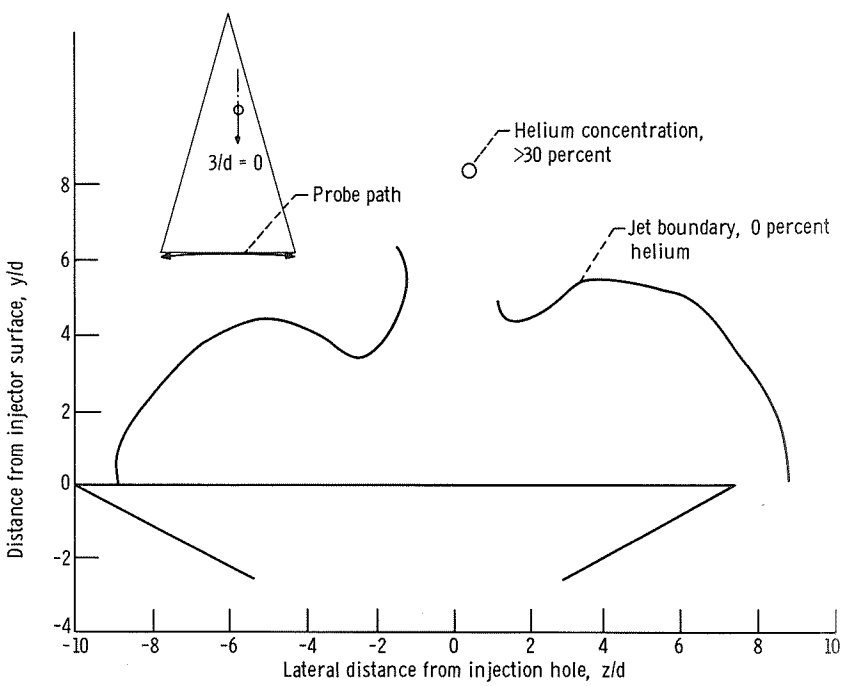

Figure 13. - Helium distribution injection from leeward surface. Distance downstream from injector orifice, 19.8; symmetrical delta-wing injector; sweepback angle, 75°; angle of attack, 22°.

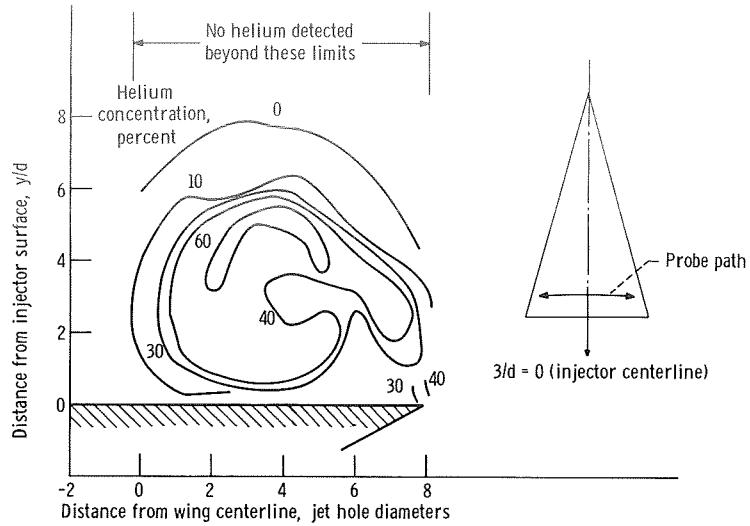

(a) Distance downstream from injector orifice, 15.9.

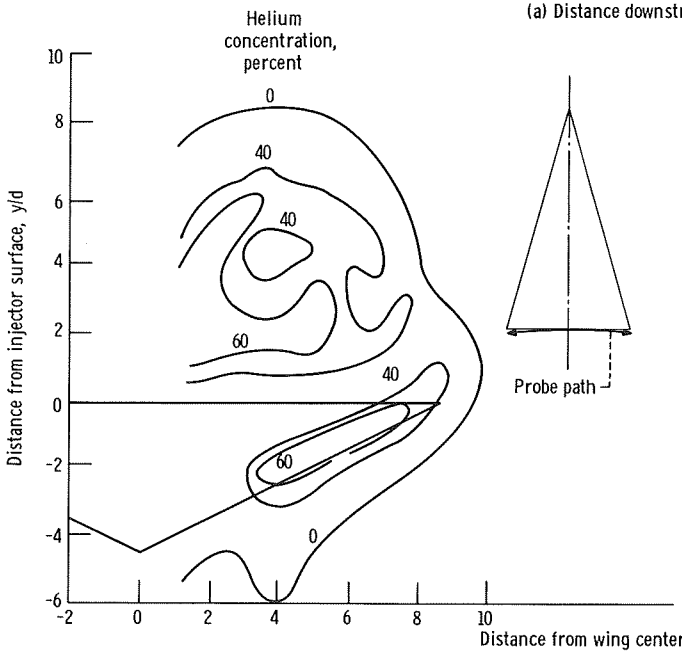

(b) Distance downstream from injector orifice, 19.5.

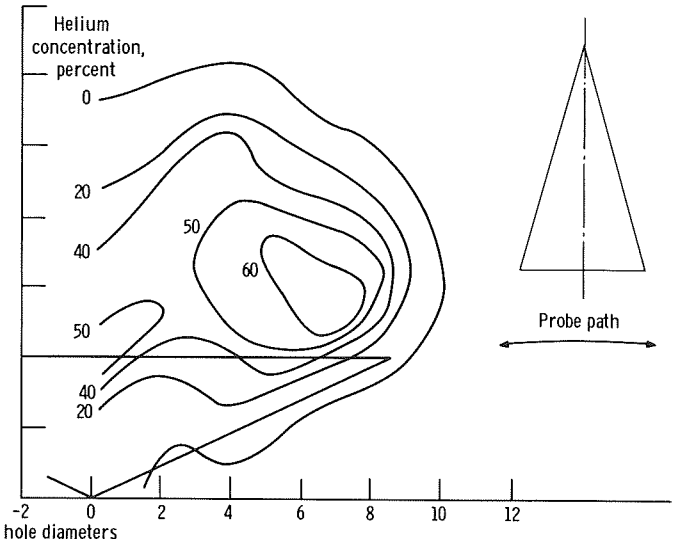

(c) Distance downstream from injector orifice, 29.5.

Figure 14. - Helium distribution. Injection from porous strip on windward surface; symmetrical delta injector; sweepback angle, 75^{0}; angle of attack, 22^{0}.

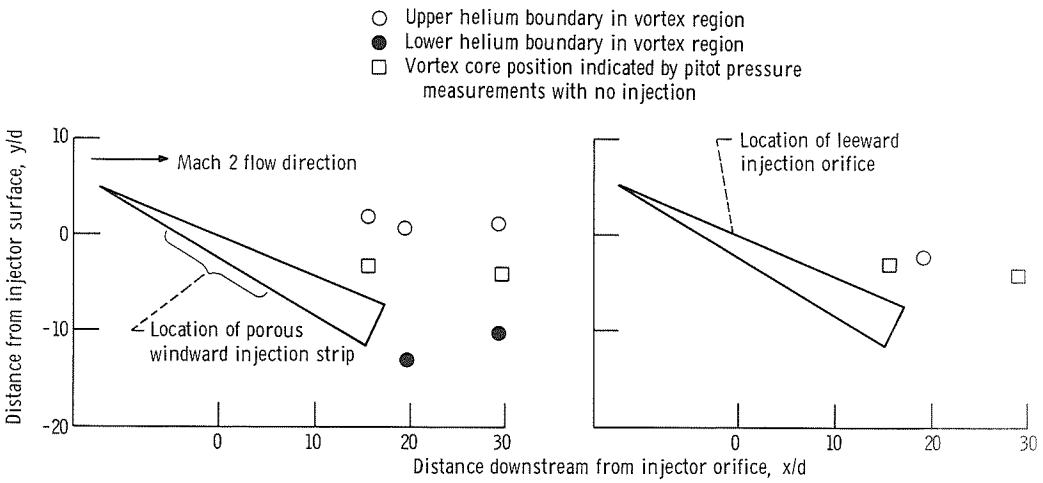

(a) Windward injection from porous strip.

(b) Leeward injection from sonic orifice.

Figure 15. - Comparison of helium penetration in vortex region with windward injection from porous strip and leeward injection from sonic orifice. Symmetrical full delta injector; sweepback angle, 75°; angle of attack, 22°.

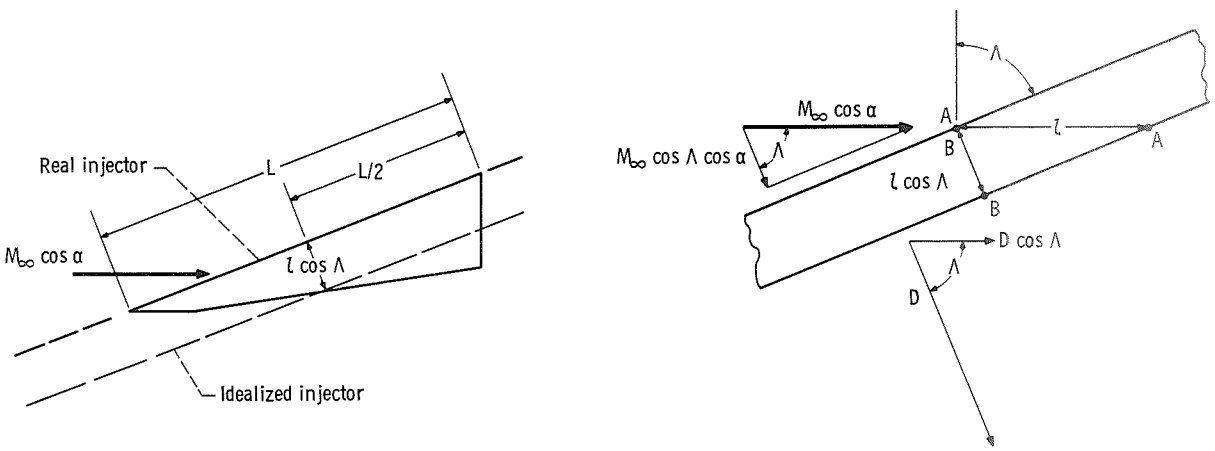

(a) Injector approximation.

(b) Infinite wing, plan view.

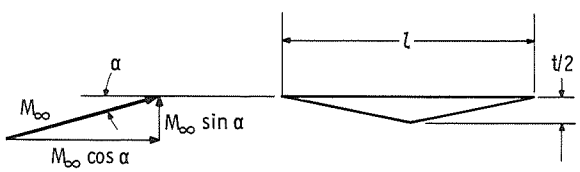

(c) Plane in direction A-A.

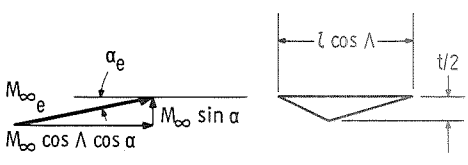

(d) Plane in direction B-B.

Figure 16. - Infinite sweptback wing (ref. 8) and injector approximation for drag calculation.

NATIONAL AERONAUTICS AND SPACE ADMINISTRATION
WASHINGTON, D. C. 20546

OFFICIAL BUSINESS
PENALTY FOR PRIVATE USE $300

FIRST CLASS MAIL

POSTAGE AND FEES PAID
NATIONAL AERONAUTICS AND
SPACE ADMINISTRATION

POSTMASTER: If Undeliverable (Section 158 Postal Manual) Do Not Return

"The aeronautical and space activities of the United States shall be conducted so as to contribute . . . to the expansion of human knowledge of phenomena in the atmosphere and space. The Administration shall provide for the widest practicable and appropriate dissemination of information concerning its activities and the results thereof."

—NATIONAL AERONAUTICS AND SPACE ACT OF 1958

NASA SCIENTIFIC AND TECHNICAL PUBLICATIONS

TECHNICAL REPORTS: Scientific and technical information considered important, complete, and a lasting contribution to existing knowledge.

TECHNICAL NOTES: Information less broad in scope but nevertheless of importance as a contribution to existing knowledge.

TECHNICAL MEMORANDUMS: Information receiving limited distribution because of preliminary data, security classification, or other reasons.

CONTRACTOR REPORTS: Scientific and technical information generated under a NASA contract or grant and considered an important contribution to existing knowledge.

TECHNICAL TRANSLATIONS: Information published in a foreign language considered to merit NASA distribution in English.

SPECIAL PUBLICATIONS: Information derived from or of value to NASA activities. Publications include conference proceedings, monographs, data compilations, handbooks, sourcebooks, and special bibliographies.

TECHNOLOGY UTILIZATION PUBLICATIONS: Information on technology used by NASA that may be of particular interest in commercial and other non-aerospace applications. Publications include Tech Briefs, Technology Utilization Reports and Technology Surveys.

Details on the availability of these publications may be obtained from:

SCIENTIFIC AND TECHNICAL INFORMATION OFFICE

NATIONAL AERONAUTICS AND SPACE ADMINISTRATION

Washington, D.C. 20546